Available online at www.sciencedirect.com
SCIENCE DIRECT®
Ore Geology Reviews 24 (2004) 299–314
ORE GEOLOGY REVIEWS
www.elsevier.com/locate/oregeorev

The effect of metasomatism on the Cr-PGE mineralization in the Finero Complex, Ivrea Zone, Southern Alps

Giovanni Grieco[a,*], Alfredo Ferrario[a], Edmond A. Mathez[b]

[a] *Dipartimento di Scienze della Terra, Università degli Studi di Milano, via Botticelli 23, 20133, Milan, Italy*
[b] *Department of Earth and Planetary Sciences, American Museum of Natural History, New York, NY 10024, USA*

Received 18 July 2001; accepted 4 May 2003

Abstract

The magmatic metasomatism that was responsible for producing chromitite–dunite bodies in the unusual phlogopite peridotite of the Finero Complex in Permian to Triassic times also influenced the Cr-platinum group elements (PGE) mineralization. At least the end stages of this metasomatism are recorded in compositional zoning of chromite grains in the podiform chromitite. Metasomatic melt, with or without vapor, reacted with chromite to produce core-to-rim Cr enrichment of extant chromite grains and was concurrent with pyroxene crystallization. Under conditions of lower melt/rock ratio, metasomatism resulted in core-to-rim Al enrichment in chromite and crystallization of amphibole between chromite and clinopyroxene. This early, high-temperature metasomatism is unrelated to the later and pervasive K-metasomatism that crystallized phlogopite and was associated with the intrusion of clinopyroxenite dikes that cut the peridotite. Much later, serpentinization of olivine locally depleted chromite in Al and enriched it in Fe and formed minor amounts of magnetite.

The PGE, which are present mainly as laurite inclusions in chromite, were remobilized by the early metasomatism. This resulted in substantial variation in the PGE contents of chromitites and imposed a characteristic PGE pattern in which chondrite-normalized Os, Ir, Ru and Rh contents are high but Pt and Pd contents are low. The slopes of PGE chondrite-normalized concentration patterns are systematically related to absolute PGE abundance and to rock mode. Chromitites with low modal orthopyroxene, clinopyroxene, and amphibole exhibit negative PGE slopes and contain relatively high PGE concentrations, whereas chromitites rich in these silicate minerals have positive slopes and low PGE contents.

Keywords: Metasomatism; Chromite; Platinum group elements; Finero; Ivrea Zone

1. Introduction

On a worldwide basis, podiform chromitites in ophiolites and Alpine-type peridotites are enriched in Os, Ir, Ru, and Rh compared to immediately adjacent rocks (e.g. Barnes et al., 1985; Ferrario and Garuti, 1987; McElduff and Stumpfl, 1990; Melcher et al., 1999), but the reasons for this enrichment are not clear (Stumpfl, 1986; Augé and Johan, 1988; Naldrett and von Gruenewaldt, 1989; Leblanc, 1991; Zhou et al., 1998). The mineral assemblage containing platinum group elements (PGE) is dominated by laurite (RuS_2, in which Os and Ir are present in solid solution), and because the PGE minerals exist almost entirely as

* Corresponding author.
E-mail address: giovanni.grieco@unimi.it (G. Grieco).

0169-1368/$ - see front matter © 2003 Elsevier B.V. All rights reserved.
doi:10.1016/j.oregeorev.2003.05.004

inclusions within chromite grains, the PGE mineralizing event is most probably related to chromite crystallization. One model for the formation of podiform chromitites and the olivine-rich rocks that invariably surround them holds that the dunite and chromitite formed by reaction of mantle peridotite with hotter melt intruded from depth (Kelemen, 1990; Kelemen et al., 1992; Leblanc and Ceuleneer, 1992; Zhou et al., 1994; Zhou and Robinson, 1997). Furthermore, although many detailed studies have found that the rocks have been substantially modified by later metasomatic processes (e.g. Agrinier et al., 1993; Arai and Yurimoto, 1994; Johnson et al., 1996; McPherson et al., 1996; Ionov et al., 1999; McInnes et al., 2001), there

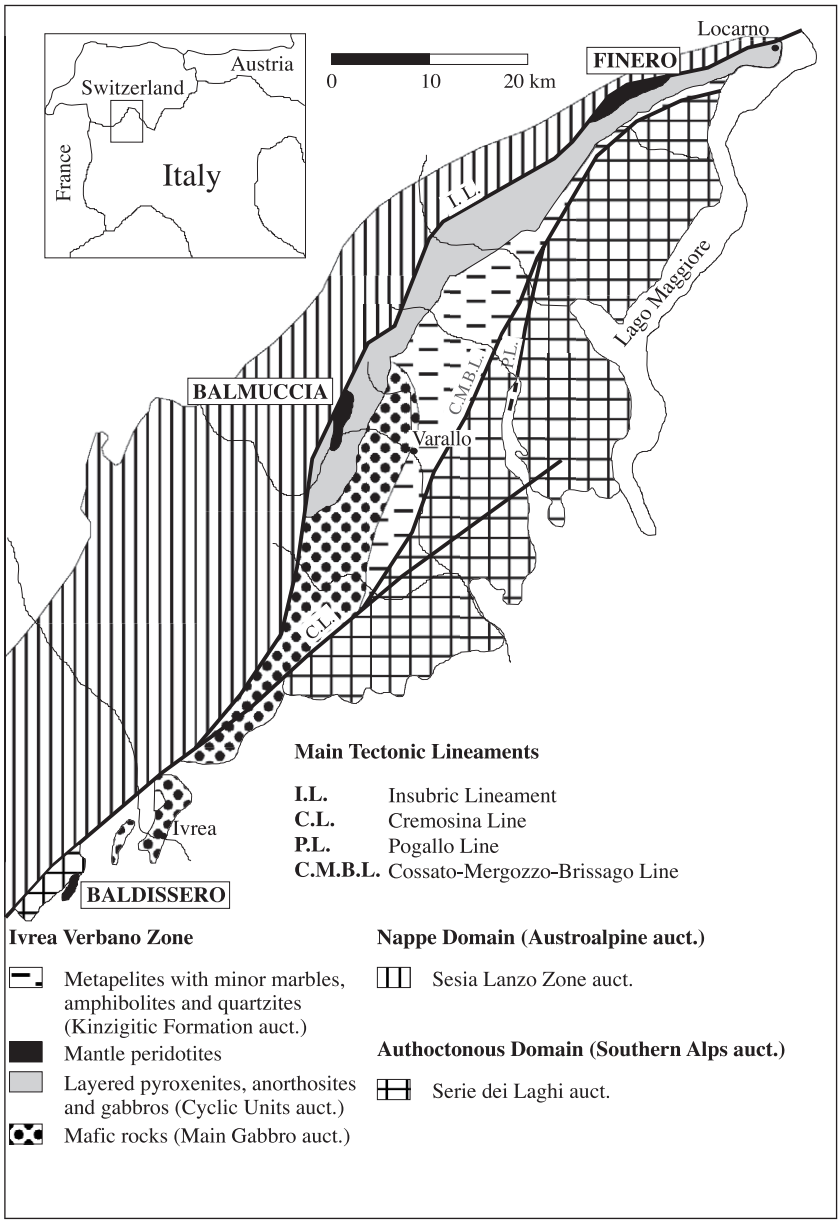

Fig. 1. Geological sketch map of Ivrea–Verbano Zone. Tectonic lineaments are shown with thick lines.

has been little investigation of how these processes relate to PGE mineralization. The Finero complex, where the dunite and chromitite appear to have formed by reaction of peridotite and melt (Grieco et al., 2001), offers a good opportunity to explore the influence of metasomatism on PGE mineralization.

2. Geology and petrography

The Finero complex lies within the Ivrea–Verbano Zone (Fig. 1), a slice of lower crustal rocks of the African plate accreted onto the European plate during the Alpine orogenesis (Nicolas et al., 1990). The Ivrea–Verbano Zone is mainly pelitic and contains rocks ranging from kinzigites of the amphibolite facies to stronalites of the granulite facies. However, many mafic–ultramafic bodies, including the Finero, Balmuccia and Baldissero complexes, exist along the western edge of the zone. To the west, the Finero complex abuts the Sesia Lanzo zone of the Austro-alpine domain across the Canavese lineament (Fig. 2), a portion of the fault system separating the Alpine and South-alpine domains. On the eastern side, it is in contact with metapelite, amphibolite and quartzite of the Kinzigite Formation.

The Finero complex is an elliptical body 12 km long and 3 km wide (Fig. 2). It comprises four main units (Coltorti and Siena, 1984) from core to rim:

1. Phlogopite peridotite—amphibole and phlogopite-bearing harzburgite to dunite containing decimeter to meter size pods of chromitite surrounded by dunite and cm- to dm-wide clinopyroxenite dikes.
2. Layered internal zone—alternating cm- to dm-thick cumulate layers of gabbro, amphibole- to garnet-bearing gabbro, websterite, clinopyroxenite, hornblendite and anorthosite.
3. Amphibole peridotite—cumulate layers of amphibole lherzolite with minor dunite and wherlite.
4. External gabbro—amphibole- to garnet-bearing massive gabbro with rare anorthosite layers.

The occurrence of chromitite in the Finero phlogopite peridotite was described by Roggiani (1948), Medaris (1975) and Forbes et al. (1978). Grieco

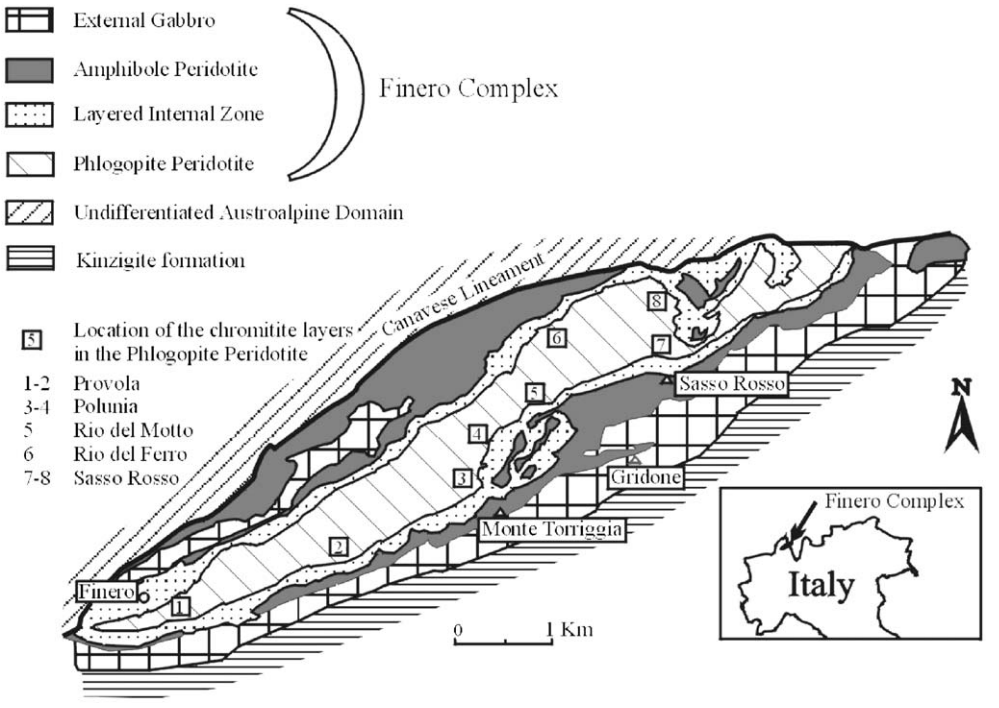

Fig. 2. Geological map of the Finero complex, with location of the chromitite outcrops. Canavese tectonic lineament is shown with a thick line.

(1998a,b) noted three petrographically and compositionally distinct Cr-bearing spinels: (a) disseminated Cr-spinel in the harzburgite, (b) chromite within the massive chromitites and (c) chromite in chromite + phlogopite symplectites. As with nearly all such occurrences, the Finero chromitites are enriched in PGE (Ferrario and Garuti, 1990; Garuti et al., 1995).

The phlogopite peridotite is an unusual rock that has attracted much attention. It is magnesium-rich, with a whole rock MgO content of 44.0 ± 1.4% and 74% modal olivine of Fo_{90-92} (Coltorti and Siena, 1989; Hartmann and Wedepohl, 1993), and is therefore believed to be a residue of partial melting (Hartmann and Wedepohl, 1993). Yet it also contains substantial amounts of phlogopite and was therefore metasomatized (Exley et al., 1982). In addition to the growth of phlogopite and other new phases (clinopyroxene, three generations of amphibole, apatite, zircon), metasomatism enriched the peridotite in incompatible trace elements (K, Na, LREE, Rb, Ba) and radiogenic Pb, and imposed a variable Nd isotopic composition (Voshage et al., 1987; Hartmann and Wedepohl, 1993; Lu et al., 1997b). In some places, localized bodies of dunite + chromitite developed and were later cut by clinopyroxenite dikes.

Exactly when the phlogopite-bearing rocks were metasomatized is unclear. The surrounding magmatic rocks are early Paleozoic (533 ± 20 Ma for the amphibole peridotite and 549 ± 12 Ma for the layered internal zone—Lu et al., 1997b), but ages obtained on the peridotite range from 293 to 163 Ma (Hunziker, 1974; Voshage et al., 1987; Hartmann and Wedepohl, 1993; Lu et al., 1997b; Grieco et al., 2001). This suggests that the peridotite experienced multiple metasomatic events that seemingly spanned tens of millions of years.

Beginning with the pioneering work of Exley et al. (1982), the complex metasomatic history at Finero has received much attention. Voshage et al. (1987), based on mixing curves for Sr versus Nd isotopes, attributed the metasomatism to crustal contamination during uplift and emplacement at shallow depth. Cumming et al. (1987) suggested that metasomatism occurred in the mantle before uplift and involved subducted crustal material. Voshage et al. (1988) advocated early deep-mantle metasomatism that resulted in the growth of amphibole, and later shallower metasomatism that involved infiltration of crustal fluids and thereby induced the formation of phlogopite. Hartmann and Wedepohl (1993) remained uncertain: they proposed that either there were two metasomatic events, or there was one protracted event involving progressively smaller volumes of increasingly incompatible element-rich contaminant. They considered that the metasomatism was triggered by subduction of crustal material and occurred deep in the mantle during the initial stages of slab-uplift. Lu et al. (1994, 1997a,b) compared the phlogopite peridotite and the surrounding magmatic sequence. They showed that the peridotite has a strong crustal isotopic signature that is lacking in the magmatic sequence. These observations, together with the contrasting dates (above), established that the magmatic sequence was not affected by the peridotite-modifying metasomatism and thereby implied that the two groups of rocks are not genetically related.

The most recent investigations are those of Zanetti et al. (1999), Garuti et al. (2000) and Grieco et al. (2001). Zanetti et al. (1999) proposed that the phlogopite peridotite was modified in a single metasomatic event that also gave rise to the clinopyroxenite dikes.

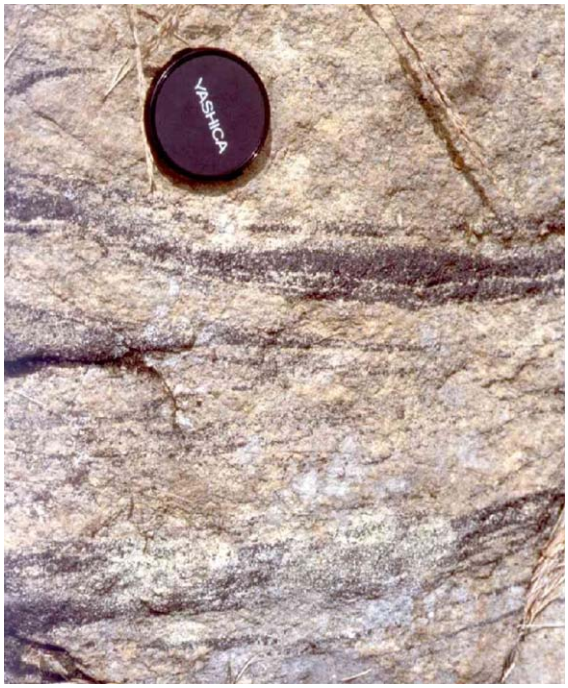

Fig. 3. An outcrop of the chromitite + dunite association at Alpe Polunia. Chromitite makes up irregular lenses, some centimeters thick.

Table 1
Representative core–rim analyses of chromite (wt.%) from Finero Phlogopite Peridotite

Contact mineral	Ol		Opx		Cpx		Cpx		Ol		Opx		Opx		Ol		Cpx	
Sample site	Core	Rim	Core	Rim	Core	Rim	Core	Rim	Core	Rim	Core	Rim	Core	Rim	Core	Rim	Core	Rim
Location	1		1		1		1		2		2		2		3		4	
SiO_2	<mdl	<mdl	<mdl	<mdl	0.05	0.05	<mdl	<mdl	<mdl	<mdl	<mdl	0.34	<mdl	<mdl	<mdl	0.89	<mdl	0.11
TiO_2	0.66	0.44	0.49	0.24	0.67	0.39	0.49	0.41	0.49	0.47	0.47	0.24	0.53	0.50	0.63	0.39	0.36	0.23
Al_2O_3	16.92	19.35	15.88	8.52	17.09	11.77	15.88	12.54	15.88	18.43	18.86	11.59	16.66	15.73	15.90	17.54	18.23	13.62
Cr_2O_3	50.03	47.46	48.11	58.00	50.07	55.85	48.11	51.18	48.11	46.11	46.32	54.11	48.47	49.80	50.31	47.28	45.57	51.27
Fe_2O_3	5.07	5.25	5.93	3.26	4.67	4.13	5.93	5.52	5.93	5.75	6.74	5.70	6.14	5.88	2.92	1.89	6.16	4.59
FeO	17.11	16.49	17.81	20.00	16.90	17.00	17.81	18.22	17.81	16.82	18.20	20.17	18.20	18.86	17.09	17.84	17.44	18.46
MnO	0.31	0.26	0.27	0.30	0.30	0.32	0.27	0.24	0.27	0.27	0.31	0.38	0.33	0.32	0.33	0.40	0.29	0.29
NiO	0.15	0.11	<mdl	<mdl	0.19	<mdl	<mdl	<mdl	<mdl	<mdl	0.05	0.08	0.09	0.06	0.12	<mdl	<mdl	<mdl
MgO	12.06	12.60	10.87	8.45	12.19	11.00	10.87	9.80	10.87	11.80	11.53	9.49	11.09	10.67	11.19	11.26	11.24	9.73
CaO	<mdl	<mdl	<mdl	<mdl	<mdl	0.32	<mdl	0.24	<mdl	<mdl	<mdl	<mdl	<mdl	<mdl	<mdl	<mdl	<mdl	0.30
Na_2O	<mdl	<mdl	<mdl	<mdl	<mdl	<mdl	<mdl	<mdl	<mdl	<mdl	<mdl	<mdl	<mdl	<mdl	<mdl	<mdl	<mdl	<mdl
K_2O	<mdl	<mdl	<mdl	<mdl	<mdl	<mdl	<mdl	<mdl	<mdl	<mdl	<mdl	<mdl	<mdl	<mdl	<mdl	<mdl	<mdl	<mdl
Total	102.31	101.96	99.36	98.77	102.13	100.83	99.36	98.15	99.36	99.65	102.48	102.10	101.51	101.82	98.49	97.49	99.29	98.60

Contact mineral	Opx		Cpx		Cpx		Ol		Cpx		Ol		Opx		Ol		Ol	
Sample site	Core	Rim	Core	Rim	Core	Rim	Core	Rim	Core	Rim	Core	Rim	Core	Rim	Core	Rim	Core	Rim
Location	4		4		4		4		4		5		6		7		8	
SiO_2	<mdl	0.14	0.06	0.08	<mdl	0.05	0.06	0.06	<mdl	0.07	<mdl	<mdl	<mdl	<mdl	<mdl	<mdl	<mdl	<mdl
TiO_2	0.52	0.40	0.34	0.28	0.28	0.21	0.34	0.44	0.25	0.18	0.66	0.51	0.67	0.50	0.25	0.25	0.59	0.71
Al_2O_3	13.05	13.97	18.70	14.49	18.57	14.27	18.97	23.42	17.57	12.90	15.68	14.86	16.62	14.81	17.6	15.4	13.86	15.33
Cr_2O_3	54.88	54.17	46.00	50.05	46.74	51.23	46.06	40.33	47.21	53.49	52.66	52.87	49.65	52.33	47.2	48.4	51.71	50.75
Fe_2O_3	2.43	1.54	5.96	6.26	5.51	4.72	5.93	6.83	5.73	4.20	3.12	3.39	5.27	4.78	5.73	5.77	5.93	6.07
FeO	18.74	19.22	17.74	17.92	17.92	18.25	18.15	17.65	17.37	17.56	17.96	17.51	17.02	16.66	17.4	18.9	17.12	17.1
MnO	0.34	0.34	0.27	0.36	0.27	0.26	0.27	0.26	0.28	0.25	0.40	0.35	0.33	0.31	0.28	0.34	0.30	0.27
NiO	0.13	0.16	0.16	0.07	0.09	0.09	0.19	0.08	<mdl	<mdl	0.11	0.23	0.15	0.05	<mdl	<mdl	0.22	<mdl
MgO	10.10	9.79	11.32	10.55	11.19	10.14	11.19	12.11	11.28	10.50	11.26	11.15	11.94	11.95	11.28	9.91	11.67	12.2
CaO	<mdl	<mdl	<mdl	0.18	<mdl	0.17	<mdl	<mdl	<mdl	0.18	<mdl	<mdl	<mdl	<mdl	<mdl	0.10	<mdl	<mdl
Na_2O	<mdl	<mdl	<mdl	<mdl	<mdl	<mdl	<mdl	<mdl	<mdl	<mdl	<mdl	<mdl	<mdl	<mdl	<mdl	<mdl	<mdl	<mdl
K_2O	<mdl	<mdl	<mdl	<mdl	<mdl	<mdl	<mdl	<mdl	<mdl	<mdl	<mdl	<mdl	<mdl	<mdl	<mdl	<mdl	<mdl	<mdl
Total	100.19	99.73	100.55	100.24	100.57	99.39	101.16	101.18	99.69	99.33	101.85	100.87	101.65	101.39	99.74	99.07	101.40	102.43

Location numbers as in Fig. 2.

They contended that the peridotite was infiltrated by melt from the subducted eclogite-facies slab, and that the clinopyroxenite dikes represent melt-dominated areas in the melt–rock mush. Garuti et al. (2000) studied ultramafic pipes in the Ivrea zone and advocated a deep-mantle source for the fluid that contaminated the pipes and phlogopite peridotite. Grieco et al. (2001), based on detailed field and petrologic studies, contended that there were two genetically distinct metasomatic events separated in time. The dunite + chromitite pods formed during the first event that also resulted in widespread amphibole crystallization and LREE enrichment in the harzburgite. A Pb–Pb age on zircon separated from chromitite dates the early metasomatism as 207.9 + 1.7 – 1.3 Ma. The unrelated second event involved pervasive K metasomatism, crystallization of phlogopite, and formation of the clinopyroxenite dikes.

3. Microanalytical study

3.1. Analytical methods

Chromite was analyzed using the ARL-SEMQ microprobe at the University of Milan. Operating conditions were 15-kV acceleration voltage, 20-nA beam current, and 3-μm spot size. Elemental determinations were made under similar operating conditions on the CAMECA SX100 microprobe at the American Museum of Natural History. For both instruments, minimum detection limits are 0.05%. PGE whole rock analyses were carried out at ACTLABS Laboratories, Canada, using preconcentration by NiS fire assay and final determination by instrumental neutron activation analysis (INAA); detection limits (in ppb) for Os, Ir, Ru, Rh, Pt and Pd were 2, 0.1, 5, 0.2, 5 and 2, respectively.

3.2. Chromitites

Podiform chromitites with haloes of dunite are well-known and common features of Alpine-type

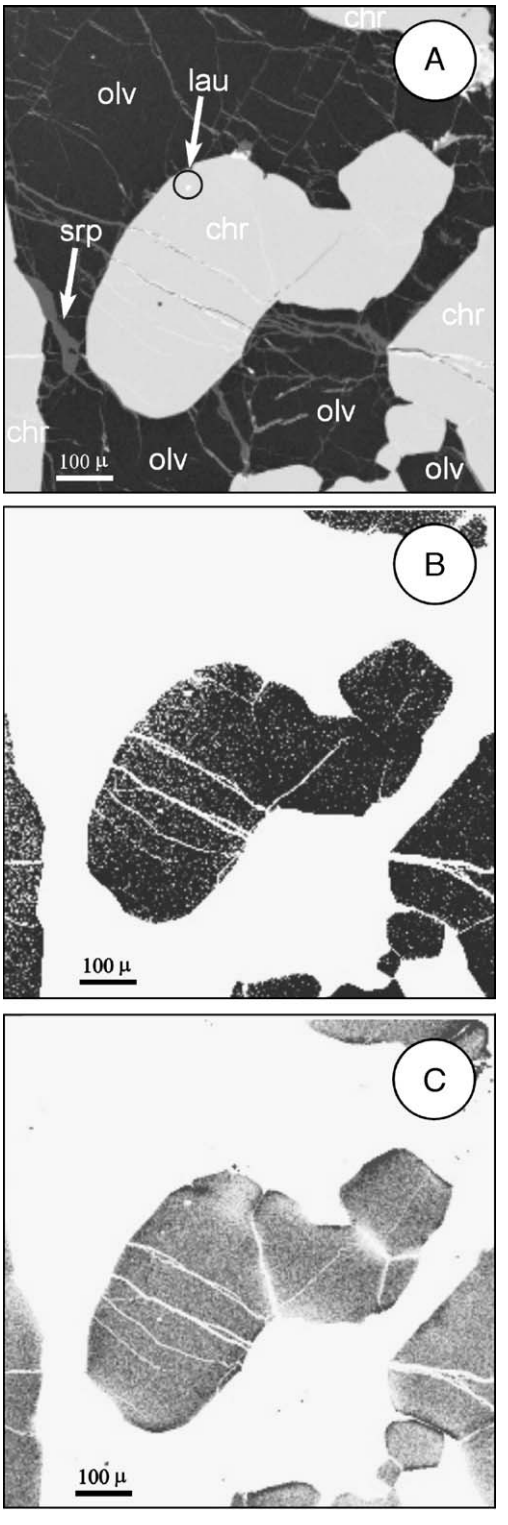

Fig. 4. Elemental maps of chromite grain in of an orthopyroxene-poor and clinopyroxene- and amphibole-free chromitite. (A) BSE image; (B) Cr distribution; (C) Al distribution. Note the laurite inclusion (circle and arrow).

peridotites. Kelemen et al. (1992) argued that dunite–harzburgite bodies formed by magma reacting with the surrounding lherzolite. The reaction is driven by the facts that melt, originally in equilibrium with a mantle mineral assemblage at depth, is saturated only in olivine upon intrusion to higher levels and hotter than the surrounding rocks. The melt thus reacts with clinopyroxene and orthopyroxene of the host lherzolite to produce olivine. With cooling to the temperature of the lherzolite, the melt continues to react with clinopyroxene to form orthopyroxene and olivine until chemical equilibrium is achieved. Zhou et al. (1994) and Zhou and Robinson (1997) extended the process to the formation of chromitites by pointing out that the dissolution of pyroxene drives olivine-saturated melt into the field of chromite stability. Massive chromitites form where extensive reaction of magma and the wall rock took place.

The field and geochemical relations of the Finero chromitites are consistent with the process suggested by Zhou et al. (1994). Despite the poor exposure, numerous chromitite bodies have been found in the phlogopite peridotite (Fig. 2). The best outcrops are those at Alpe Polunia, in the central portion of the body, next to the southern border. The chromitites form lenses, discontinuous layers and pods up to 40 cm thick and 50 m long, that are generally encompassed by dunite haloes extending centimeters to meters from the chromitite (Fig. 3). The dunite–chromitite assemblage, which represents the melt-dominated portion of the crystal mush, grades into the host peridotite.

Chromite of the massive chromitites was studied to gain insight into the metasomatism that presumably represented the final stages of the process of podiform chromitite–dunite formation. A series of core–rim analyses of chromite grains show that the nature of chemical zoning (Table 1) is related to the particular contact silicate mineral. In fact, individual chromite grains show different core–rim zoning when in contact with more than one mineral type. Chromite in contact with olivine is unzoned or the rims contain slightly less

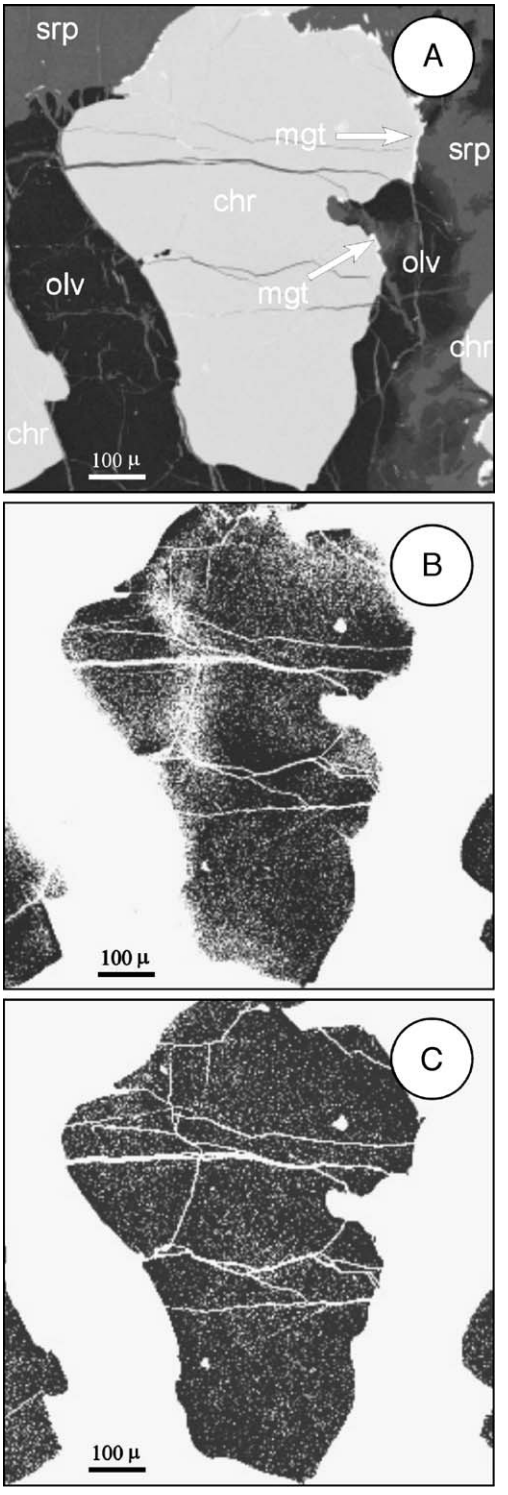

Fig. 5. Elemental maps of chromite grain in a partially serpentinized, orthopyroxene-poor and clinopyroxene- and amphibole-free chromitite. (A) BSE image; (B) Cr distribution; (C) Al distribution. Arrows point at small overgrowth of magnetite on chromite.

Cr and more Al than the cores. In contrast, rims in contact with orthopyroxene and clinopyroxene are enriched in Cr_2O_3 and depleted in Al_2O_3 by up to 10% compared to their respective cores. These rims also exhibit minor (usually less than 2 wt.%) enrichment in Fe^{2+} and depletion in Mg. Finally, rims in contact with amphibole are always enriched in Al and depleted in Cr. The zoning patterns are illustrated by distribution maps for Cr and Al (Figs. 4–7).

In chromite–olivine rocks, the chromite is homogeneous or exhibits only slight rim enrichments in Al and Fe and depletions in Cr and Mg (Figs. 4 and 5; note that the grain of Fig. 4 also contains an inclusion of laurite, the most common PGE chromitite mineral). Serpentinization is limited to late fractures. The grain in Fig. 5, approximately 30 cm from that in Fig. 4, is unzoned, but serpentinization is far more extensive. Again serpentinization is related to two orientations of fractures (E–W and N–S in the map). The chromite grain shows an overgrowth of magnetite and depletion in Al on the right border. Depletion in Al, not balanced by enrichment in Cr, is also present around the N–S fractures.

Fig. 6 shows a sample containing orthopyroxene and olivine. The chromite grain is unzoned except in the lower left side, where it is in contact with orthopyroxene and shows a slight enrichment in Cr and depletion in Al. This zoning is opposite to that in Fig. 4 and in regions of the same grain in contact with olivine.

Fig. 7 is of one of the samples where metasomatism proceeded further and resulted in crystallization of clinopyroxene and pargasitic amphibole. Zoning is complex and more extensive than elsewhere. Rims in contact with both orthopyroxene and clinopyroxene are strongly enriched in Cr and depleted in Al, but rims in contact with olivine and amphibole are enriched in Al and depleted in Cr. Strong enrichment in Cr and depletion in Al is also observed around a fracture within the chromite grain. The two color maps of Fig. 8 emphasize the nature of the zoning and thereby endorse the observations made about Fig. 7. Fig. 8A shows the variation of Cr/Al ratio, while Fig. 8B shows thin

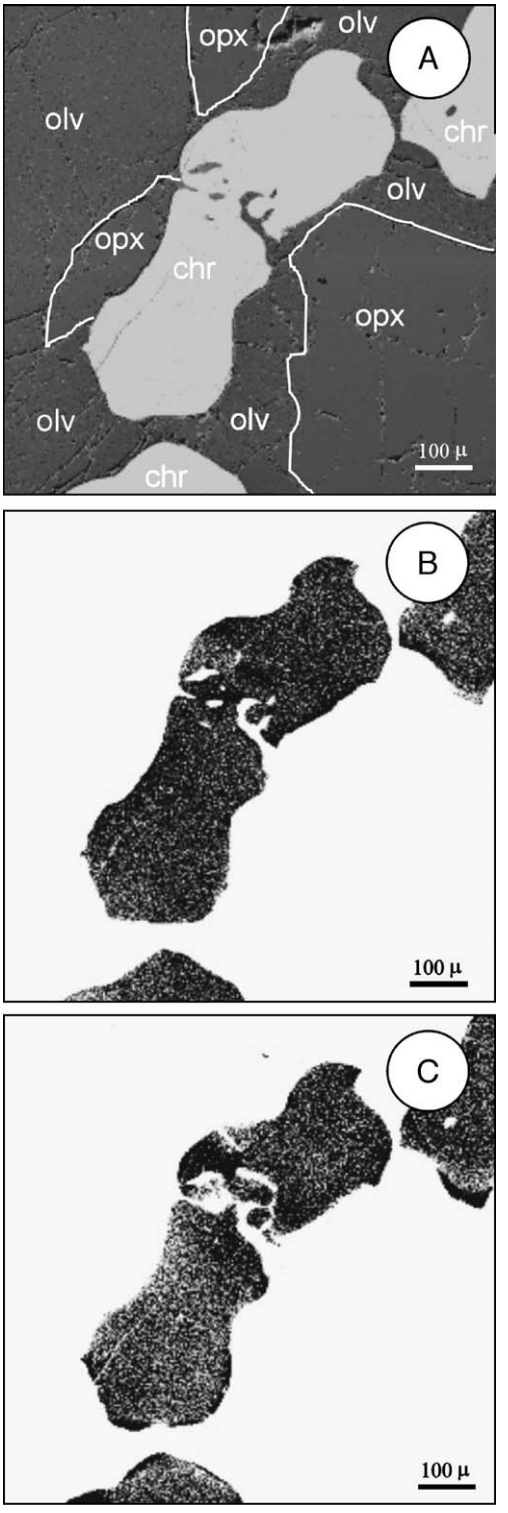

Fig. 6. Elemental maps of chromite grain in an orthopyroxene-rich and clinopyroxene- and amphibole-poor chromitite. (A) BSE image; (B) Cr distribution; (C) Al distribution.

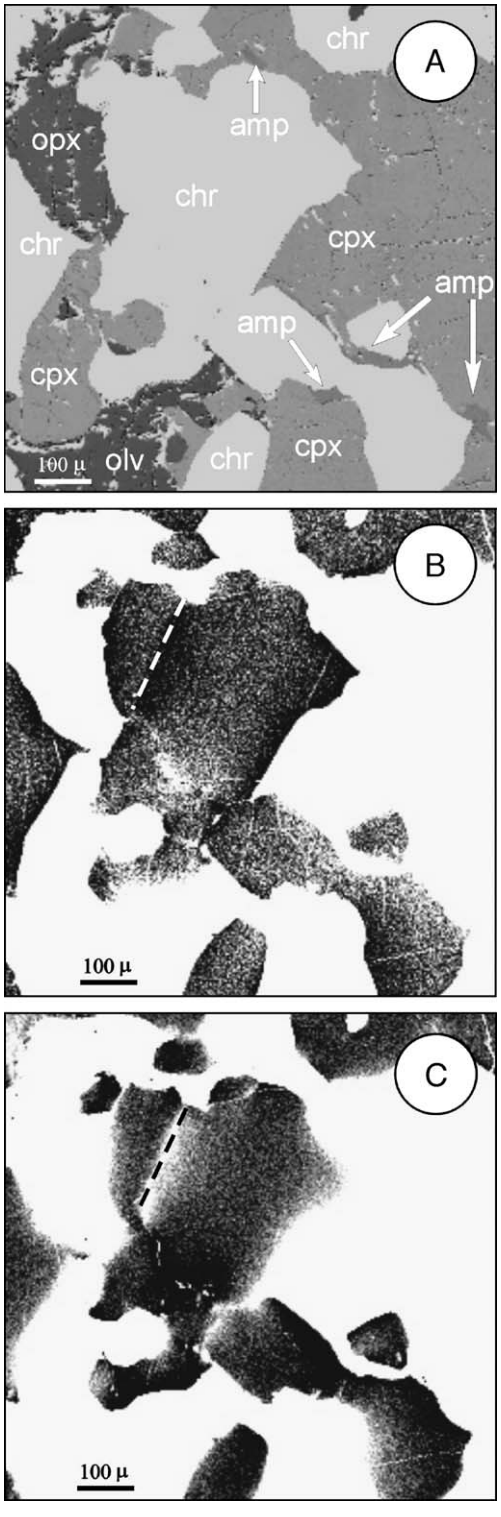

Fig. 7. Atomic maps of chromite grain in orthopyroxene-, clinopyroxene-, and amphibole-rich chromitite. (A) BSE image; (B) Cr distribution; (C) Al distribution. Hatched line marks a fracture.

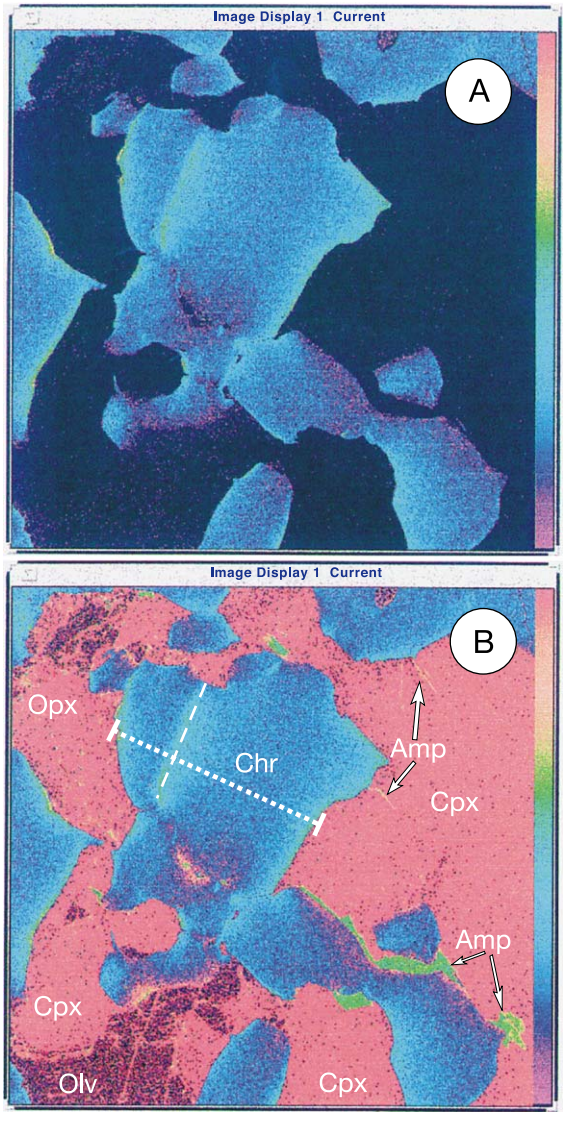

Fig. 8. Calibrated (A) and non-calibrated atomic maps of the chromite grain of Fig. 6. The maps emphasize chromite zoning and show the presence of thin amphibole films within cleavage planes of clinopyroxene. Hatched line marks a fracture.

amphibole plates along the clinopyroxene cleavage planes.

Finally, a traverse across a chromite grain and enclosed fracture (Fig. 9) is from a rim in contact

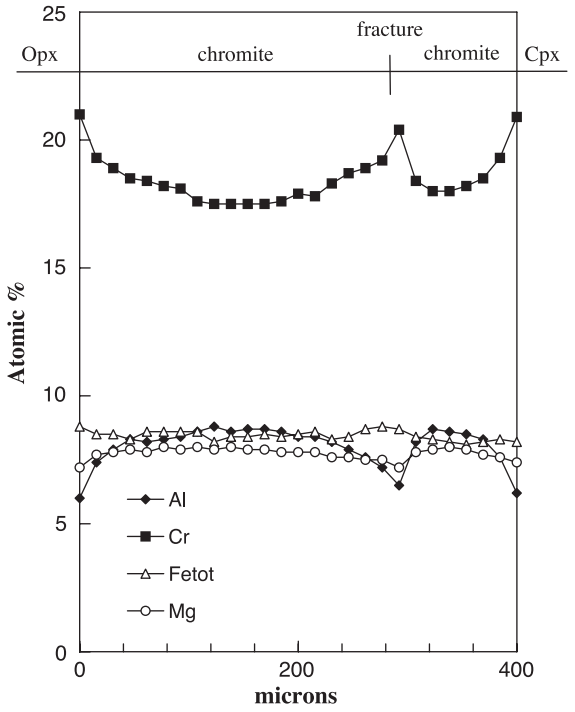

Fig. 9. Distribution of Cr, Al, Mg and Fe along a traverse within the chromite grain of Fig. 8.

with orthopyroxene to a rim in contact with clinopyroxene. The zoning for the elements shown is similar adjacent to both rims and also the fracture.

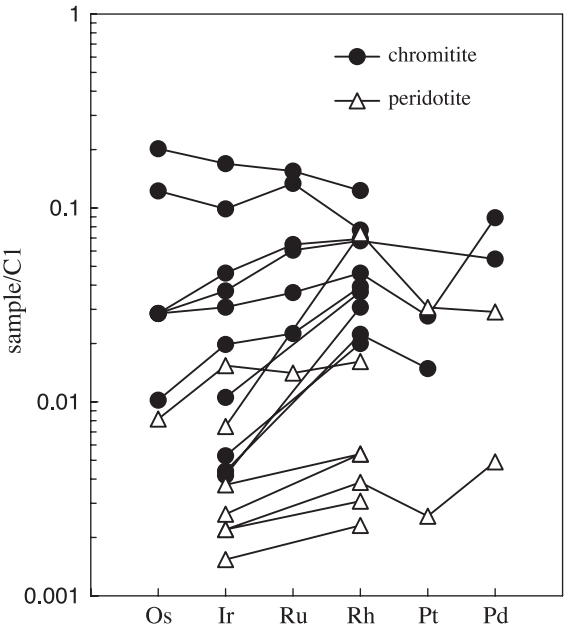

Fig. 10. Chondrite-normalized PGE patterns of chromitite and peridotite. Normalizing values are from Anders and Grevesse (1989).

3.3. Platinum group elements

The Finero chromitite bodies contain highly variable amounts of PGE. Thus, the whole rock PGE

Table 2
Whole rock PGE analyses (in ppb) from peridotite, chromitite and clinopyroxenite

Lithology	Peridotite								Chromitite									
Location									1	2	2	3	3	3	4	4	4	4
Os	4.0	<2	<2	<2	<2	<2	<2	<2	<2	<2	<2	14.0	99	14	5.0	<2	<2	14
Ir	7.0	0.7	0.9	1.0	1.7	1.2	3.4	1.0	2.4	0.9	1.3	21.0	77	17	9.0	4.8	2.0	4.0
Ru	10	<5	<5	<5	<5	<5	<2	<5	<5	<5	5.0	46.0	110	43	16.0	<5	<5	<5
Rh	2.1	0.3	0.9	0.5	0.7	0.7	9.6	0.4	2.6	<0.1	<0.1	9.0	16	8.8	5.1	4.8	2.9	7.0
Pt	<5	<5	<5	2.6	0.7	0.8	31.0	0.9	1.5	<5	<5	<5	<5	<5	<5	<5	15.0	<5
Pd	<2	<2	<2	2.7	0.3	0.9	16.0	0.4	0.2	<2	<2	<2	<2	30	<2	<2	<2	<2

Lithology	Chromitite															Clinopyroxenite		
Location	4	4	4	4	5	5	5	5	5	6	6	7	7	8	8			
Os	60	<2	<2	<2	<2	6.0	4.0	<2	<2	9.4	<2	<2	<2	14	<2	<2	<2	
Ir	45	1.9	1.1	2.5	8.0	2.0	5.0	3.0	5.0	5.4	3.2	1.1	5.6	14	2.3	0.1	0.1	
Ru	95	<5	<5	10.0	13	<5	9.0	16	<5	<5	<5	<5	<5	26	<5	<5	<5	
Rh	10	4.0	1.1	1.3	9.0	3.0	7.0	6.0	7.0	1.6	4.3	6.0	4.4	6.0	2.4	0.3	0.2	
Pt	<5	<5	16.0	5.0	<5	<5	<5	<5	<5	<5	31	<5	<5	28	<5	<5	<5	
Pd	<2	<2	<2	<2	<2	<2	<2	<2	<2	<2	120	<2	<2	49	<2	<2	4.0	

Location numbers for chromitites as in Fig. 2.

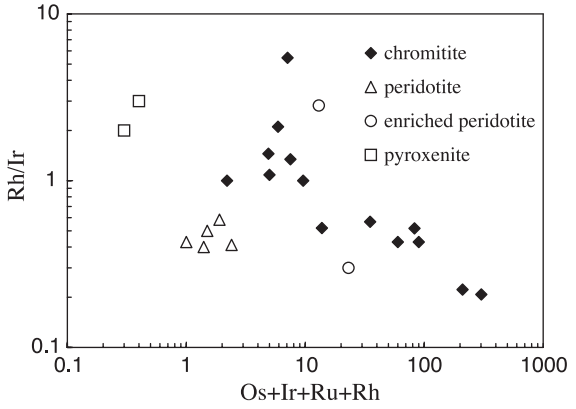

Fig. 11. Plot of Os + Ir + Ru + Rh content versus Rh/Ir ratio.

content of hand specimens ranges from less than 10 ppb to more than 300 ppb, with most samples containing less than 100 ppb (Table 2). Laurite is the main PGE phase, but cuprorhodsite (RhCuS), cuproiridsite (IrCuS), Rh–Pb alloy, Rh–Cu alloy, and minor amounts of PGE are present in pentlandite and millerite (Ferrario and Garuti, 1990; Garuti et al., 1995). Most PGE minerals occur as inclusions within chromite, but a few laurite grains were found at chromite-silicate boundaries or enclosed by olivine (Ferrario and Garuti, 1990). The miniscule quantities of Pt and Pd in the rocks (see below) are present as minor components in thiospinels. Malanite, the Pt thiospinel, was not encountered, despite being common in the Ojèn chromitites (Garuti et al., 1995). Base metal sulfides, which include pentlandite, millerite, heazlewoodite and minor chalcopyrite, chalcocite, covellite, digenite and valleriite, occur as small inclusions in chromite. They are commonly associated with PGE-bearing phases and form large (hundreds of micrometers across) interstitial aggregates between chromite grains (Ferrario and Garuti, 1990). Thus, the two samples with high Pt and Pd contents contain interstitial sulfide aggregates, whereas in Pt- and Pd-poor samples, they are much less common.

Chondrite-normalized PGE patterns of chromitites (Fig. 10) show two trends. First, normalized Os, Ir, Ru and Rh contents are much greater than normalized Pt and Pd contents that are, in many cases, below analytical detection limits. However, in a few cases, there is an enrichment in Pt and Pd that is apparently unrelated to other PGE abundances. Second, Os, Ir, Ru and Rh patterns in PGE-rich samples have slightly negative slopes, while in PGE-poor samples, they are positive. This is supported by Fig. 11, where Rh/Ir (ranging from 0.21 to 9.88 and providing a measure of the slope) decreases as Os + Ir + Ru + Rh increases, despite a high dispersion at low PGE content partly reflecting analytical error near the detection limits.

The PGE data also reflect the silicate mineralogy of the chromitites (Table 3) in that modal (Opx + Cpx + Amp)/Ol correlates inversely with Os + Ir + Ru + Rh (Fig. 12A) and directly with Rh/Ir (Fig. 12B). In essence, PGE minerals are most abundant where the silicate in chromitite is mainly olivine and least abundant where the silicates are mainly orthopyroxene, clinopyroxene and amphibole. Abundant amphibole particularly indicates pervasive metasomatism.

The PGE content of the peridotites is typically less than 5 ppb total (Fig. 11). Two exceptions to this (23.1 and 60 ppb total PGE) are from highly metasomatized, amphibole-rich harzburgite next to a dunite + chromitite body.

Clinopyroxenite dykes contain less than 5 ppb total PGE and less than 0.5 ppb of Os + Ir + Ru + Rh (Table 2; Fig. 11). This suggests that they had no effect on

Table 3
Rock mode of chromitite

Location	1	3	4	4	4	4	4	6	7	8
Chromite %	61.8	74.0	66.0	66.4	64.0	52.4	59.6	76.8	70.6	47.6
Olivine	21.8	27.4	15.6	2.2	1.8	46.4	11.0	15.4	7.4	46.2
Orthopyroxene	13.2	3.2	16.4	23.8	13.2	0.0	17.2	6.8	19.4	4.4
Clinopyroxene	3.2	0.8	1.4	7.0	9.6	0.2	10.0	1.0	2.6	0.4
Amphibole	0.0	0.4	0.6	0.6	8.6	0.0	2.2	0.0	0.0	0.0
Phlogopite	0.0	0.0	0.0	0.0	2.8	0.0	0.0	0.0	0.0	1.4
Magnetite	0.0	0.0	0.0	0.0	0.0	1.0	0.0	0.0	0.0	0.0

Location numbers for chromitites as in Fig. 2.

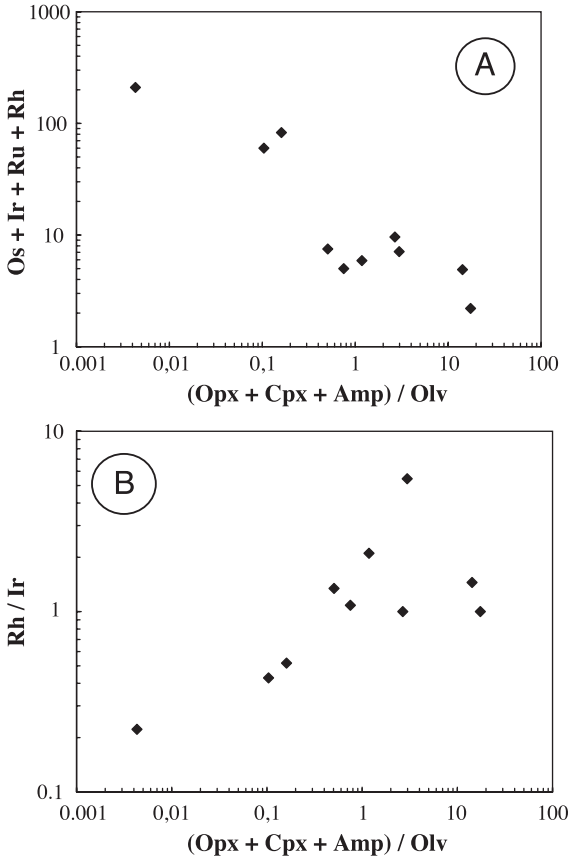

Fig. 12. Modal (Opx + Cpx + Amp)/Ol ratios of chromitites (A) versus Os + Ir + Ru + Rh contents and (B) versus Rh/Ir ratios.

anomalously high PGE distribution in metasomatized peridotite. It is of note that the dykes plot as a low PGE extension of the inverse relationship between Os + Ir + Ru + Rh and Rh/Ir in Fig. 11.

4. Discussion

4.1. Significance of zoning patterns in chromitite

Variable chromite composition is characteristic of most ophiolitic chromitite bodies (Thayer, 1964; Irvine, 1967; Leblanc and Violette, 1983; Leblanc and Nicolas, 1992), but it tends to occur between rather than within individual lenses (Leblanc and Nicolas, 1992). The variability mainly constitutes the coupled exchange between Al^{3+} and Cr^{3+} in the Y site of the spinel structure and Mg^{2+} and Fe^{2+} in the X site. The most common zoning, comprising core-to-rim depletion in Cr and Mg and enrichment in Al and Fe^{2+} (Leblanc and Ceuleneer, 1992), is an expected consequence of magmatic fractional crystallization and is consistent with the Fe and Al enrichment of chromite in the upper portions of peridotite massifs (Augé, 1987; Leblanc and Ceuleneer, 1992).

Zoning in chromite can result from plagioclase crystallization removing Al from the melt (Roeder and Reynolds, 1991), but this is obviously inapplicable to rocks devoid of plagioclase. Another cause of zoning involves reactions with interstitial melt or other fluid. For example, Neal (1988) suggested that the outward increase of Cr/(Cr + Al) in spinels in xenoliths from Malaita Island, New Caledonia, reflected leaching of Al by hydrated fluid to form pargasitic amphibole. For the Mg end-member, the reaction is:

$$\underset{\text{ChrI}}{24MgAlCrO_4} + \underset{\text{Cpx}}{16CaMgSi_2O_6} + \underset{\text{Opx}}{14Mg_2Si_2O_6}$$
$$+\underset{\text{fluid}}{8H_2O} + 4Na_2O \rightarrow \underset{\text{Amp}}{8NaCa_2Mg_4Al_3Si_6O_{22}(OH)_2}$$
$$+\underset{\text{ChrII}}{12MgCr_2O_4} + \underset{\text{Ol}}{12Mg_2SiO_4}$$

Yet another possibility is that spinel became zoned as it grew. For example, Dawson (1987) suggested that the assemblage Ti-enstatite + chromite + phlogopite + ilmenite forms locally in the mantle by reaction of water-rich fluid and Cr-diopside. Such a process could result in mineral zoning as the reaction progresses.

At Finero more than one process produced zoned chromites. Some grains in contact with olivine show a magmatic growth pattern with slight core-to-rim depletion in Cr and Mg and enrichment in Al and Fe^{2+}. Where chromite is in contact with orthopyroxene or clinopyroxene the core-to-rim zoning is reversed, with depletion in Al and enrichment in Cr. This is the same zoning pattern as observed around older fractures in chromite grains (Fig. 6), suggesting that it resulted from reaction of chromite and interstitial fluid. Furthermore, involvement of chromite in the reaction is supported by films of pargasitic amphibole between chromite and clinopyroxene and along cleavage planes in clinopyroxene (cf. Neal, 1988; above).

Although the reaction proposed by Neal (1988) explains the consumption of clinopyroxene and formation of olivine in Finero rocks, it is inconsistent with certain other observations. Thus, chromite in contact with amphibole is enriched rather than depleted in Al, thereby implying that Al in the amphibole was fluid-sourced rather than chromite-sourced, and that the fluid contributed Al to the chromite. The zoning patterns suggest the following model reaction:

$$\underset{\text{ChrI}}{4MgCr_2O_4} + \underset{\text{Cpx}}{4CaMgSi_2O_6} + \underset{\text{Ol}}{4Mg_2SiO_4} + \underset{\text{fluid}}{2H_2O} + Na_2O + 7Al_2O_3 \rightarrow \underset{\text{Amp}}{2NaCa_2Mg_4Al_3Si_6O_{22}(OH)_2} + \underset{\text{ChrII}}{8MgAlCrO_4}$$

In this reaction, chromite and amphibole form at the expense of clinopyroxene. The presence of amphibole after clinopyroxene in an assemblage containing chromite and olivine is evidence for this reaction.

The metasomatic reaction that enriched chromite in Cr at orthopyroxene and clinopyroxene contacts must pre-date the above amphibole-forming reaction, since the enrichment is related to the crystallization rather than the consumption of clinopyroxene. One possibility is that Cr-enriched rims formed due to removal of Al to form the pyroxene. The mean Al/Cr ratios of clinopyroxene and orthopyroxene are 1.78 and 3.06, respectively. In chromite, this ratio is only 0.29, and chromite is the only internal source of Al. While the presence of amphibole along intergranular boundaries and pyroxene cleavage planes argues for a very low melt/rock ratio, the granular texture of clinopyroxene and orthopyroxene suggests crystallization in the presence of a relatively high proportion of interstitial melt.

In a metasomatic system such as Finero, the compositions of the crystalline phases and interstitial melt probably evolved with time in response to changing variables such as temperature. At any one time, however, substantial gradients probably existed in interstitial melt composition depending on the nature of the surrounding solid assemblage. The continued reequilibration of interstitial melt with the solid assemblage through space and time could account for the complex zoning of the chromite. For example, crystallization of chromite would have caused Cr depletion in adjacent interstitial melt, olivine crystallization would have increased melt Cr content, and pyroxene cyrstallization would have depleted the melt in Al. Whether these reactions occurred in sequence or together cannot be ascertained solely from observations on zonation and textures, but it is clear that the processes involved in chromite zonation do not require the input of crustal material.

The latest event that modified zoning of chromite grains is recorded in the grain of Fig. 4, where chromite immediately adjacent to fractures is depleted in Al with no enrichment in Cr. Elsewhere in the same grain, the late growth of magnetite, a common feature in podiform chromitites, is associated with Al depletion (Fig. 5). This presumably reflects chromite reequilibration during serpentinisation at low temperature; it was the last metasomatic event to modify the rocks. Neither the K-metasomatism that produced phlogopite, nor the concomitant intrusion of clinopyroxene dikes affected chromite composition or significantly modified the modes of chromite-rich rocks. In fact, only a few samples of chromitite contain more than trace amounts of phlogopite, and even in these, chromite compositions and zoning patterns are no different from phlogopite-free chromitite.

4.2. Distribution of PGE

Since metasomatic processes affected chromite composition, the possibility that they also influenced PGE mineralogy and distribution must be considered. The PGE are present in minor phases such as Cu-bearing sulfides and alloys, and as inclusions of laurite. Mathez (1999) pointed out that inclusions in ophiolitic chromitites could either have formed in the early stages of magmatic crystallization, or be preserved as residues of partial melting. He cited thermodynamic relations that preclude alloys and laurite from being stable in the presence of natural basaltic melts. The inclusion phases therefore appear to require processes that involve reaction between sulfide and chromite plus fluid. The extant PGE minerals could conceivably be residues from fluid-leaching of S from original base metal sulfides and incorporation of Fe and Ni into chromite (e.g. Naldrett and Lehmann, 1988).

Two observations at Finero indicate that metasomatism influenced PGE distribution and that the mineralization is related to the development of the lithology. The first is that the PGE minerals are concentrated in chromitites that have olivine as the dominant silicate phase. PGE minerals either never existed in the pyroxene-bearing chromitites, or they were dissolved out by metasomatic reactions. Anomalously high PGE enrichment in only one sample of peridotite is consistent with PGE transport by the mobile phase. The second is that PGE normalized slopes are negative in chromitites with low modal orthopyroxene, clinopyroxene and amphibole, and positive in orthopyroxene-, clinopyroxene- and amphibole-rich chromitites. This implies that metasomatic processes affected PGE in the order Os>Ir>Ru>Rh. However, the mechanism of PGE remobilization is speculative, at least partly because the composition of the fluid phase(s) is unknown. One possibility is that PGE were dissolved as chlorate complexes, since Cl is a relatively abundant minor element in metasomatized peridotites (Kislov et al., 1997).

5. Conclusions

The study of chromite zonation provides some insight into the processes that affected Cr-PGE mineralization at Finero; it indicates that the mineralization was influenced by various types of metasomatism. First, early interaction between chromite and interstitial melt or other fluid depleted chromite in Al and enriched it in Cr, while interaction of chromite with lesser amounts of Al-rich melt or other fluid produced a reversed zonation whereby chromite rims were enriched in Al. These two reactions resulted in the formation of articulated mosaic zoning in chromite, but they did not substantially change the whole rock content of Cr. In contrast, the same metasomatic event had a much more consistent effect on PGE content. Observations argue for remobilization of PGE at least on the centimeter- to meter-scales. The total PGE of individual rocks was changed by an order of magnitude, while the relative proportions of the different PGE were also modified. Second, the pervasive K-metasomatism that involved crustal material and crystallized phlogopite, neither affected the dunite + chromitite assemblage, nor modified the PGE distribution. Finally, during the much later partial serpentinization of dunite, magnetite formed locally after chromite and, in the immediate vicinity of microfractures, chromite became depleted in Al and enriched in Fe.

References

Agrinier, P., Mével, C., Bosch, D., Javoy, M., 1993. Metasomatic hydrous fluids in amphibole peridotites from Zabargad Island (Red Sea). Earth and Planetary Science Letters 120, 187–205.

Anders, E., Grevesse, N., 1989. Abundances of the elements: meteoritic and solar. Geochimica et Cosmochimica Acta 53, 197–214.

Arai, S., Yurimoto, H., 1994. Podiform chromitites of the Tari–Misaka ultramafic complex, Southwestern Japan, as mantle–melt interaction products. Economic Geology 89, 1279–1288.

Augé, T., 1987. Chromite deposits in the northern Oman ophiolite: mineralogical constraints. Mineralium Deposita 22, 1–10.

Augé, T., Johan, Z., 1988. Comparative study of chromite deposits from Troodos, Vourinos, North Oman, and New Caledonia ophiolites. In: Boissonnas, J., Omenetto, P. (Eds.), Mineral Deposits Within the European Community. Springer, Berlin, pp. 267–288.

Barnes, S.J., Naldrett, A.J., Gorton, M.P., 1985. The origin of the fractionation of platinum-group elements in terrestrial magmas. Chemical Geology 53, 303–323.

Coltorti, M., Siena, F., 1984. Mantle tectonite and fractionate peridotite at Finero (Italian Western Alps). Neues Jahrbuch für Mineralogie. Abhandlungen 149, 225–244.

Coltorti, M., Siena, F., 1989. The petrogenesis of a hydrated mafic–ultramafic complex and the role of amphibole fractionation at Finero (Italian Western Alps). Neues Jahrbuch für Mineralogie Monatshefte, 255–274.

Cumming, G.L., Köppel, V., Ferrario, A., 1987. A lead isotope study of the northeastern Ivrea Zone and the adjoining Ceneri Zone (N-Italy): evidence for a contaminated subcontinental mantle. Contributions to Mineralogy and Petrology 97, 19–30.

Dawson, J.B., 1987. Metasomatized harzburgites in kimberlite and alkaline magmas: enriched restites and flushed lherzolites. In: Menzies, M.A., Hawkesworth, C.J. (Eds.), Mantle Metasomatism. Academic Press, London, pp. 125–144.

Exley, R.A., Sills, J.D., Smith, J.V., 1982. Geochemistry of micas from the Finero spinel–lherzolite, Italian Alps. Contributions to Mineralogy and Petrology 81, 59–63.

Ferrario, A., Garuti, G., 1987. Platinum-group minerals in chromite-rich horizons of the Niquelandia Complex (Central Goias, Brazil). In: Prichard, H.M., Potts, P.J., Bowles, J.F.W., Cribb, S.J. (Eds.), Geo-Platinum 87 Symposium. Elsevier, London, pp. 261–272.

Ferrario, A., Garuti, G., 1990. Platinum-group minerals inclusions in chromitites of the Finero mafic–ultramafic complex (Ivrea-Zone, Italy). Mineralogy and Petrology 41, 125–143.

Forbes, W.C., Mottana, A., Morten, L., 1978. Gigantic mineral patches in the ultramafic rocks of the Finero Complex (Central Alps). Proceedings of the 2nd Symposium Ivrea–Verbano. Memorie della Societa Geologica Italiana, vol. 33, pp. 127–133.

Garuti, G., Gazzotti, M., Torres-Ruiz, J., 1995. Iridium, rhodium, and platinum sulfides in chromitites from the ultramafic massifs of Finero, Italy, and Ojèn, Spain. Canadian Mineralogist 33, 509–520.

Garuti, G., Bea, F., Zaccarini, F., Montero, P., 2000. Age, geochemistry and petrogenesis of the ultramafic pipes in the Ivrea Zone, NW Italy. Journal of Petrology 42, 433–457.

Grieco, G., 1998a. Le mineralizzazioni a cromite e PGE del complesso di Finero: relazioni con i processi metasomatici. PhD thesis, Dipartimento di Scienze della Terra, Università degli Studi di Milano. 152 pp.

Grieco, G., 1998b. Chromite and PGE mineralizations of the Finero complex (southern Alps, Italy): relations with metasomatic processes. Plinius 19, 134–140.

Grieco, G., Ferrario, A., von Quadt, A., Koeppel, V., Mathez, E.A., 2001. The zircon-bearing chromitites of the Phlogopite Perifdotite of Finero (Ivrea Zone, Southern Alps): evidence and geochronology of a metasomatized mantle slab. Journal of Petrology 42, 89–101.

Hartmann, G., Wedepohl, K.H., 1993. The composition of peridotite tectonites from the Ivrea Complex, northern Italy: residues from melt extraction. Geochimica et Cosmochimica Acta 57, 1761–1782.

Hunziker, J., 1974. Rb–Sr and K–Ar age determination and the alpine tectonic history of the western Alps. Memorie degli Istituti di Geologia e Mineralogia dell' Università di Padova 31, 1–54.

Ionov, D.A., Gregoire, M., Prikhod, V.S., 1999. Feldspar-Ti-oxide metasomatism in off-cratonic continental and oceanic upper mantle. Earth and Planetary Science Letters 165, 37–44.

Irvine, T.N., 1967. Chromian spinel as a petrogenetic indicator: Part II. Petrologic applications. Canadian Journal of Earth Sciences 4, 71–103.

Johnson, K.E., Davis, A.M., Bryndzia, L.T., 1996. Contrasting styles of hydrous metasomatism in the upper mantle: an ion microprobe investigation. Geochimica et Cosmochimica Acta 60, 1367–1385.

Kelemen, P.B., 1990. Reaction between ultramafic rock and fractionating basaltic magma: I. Phase relations, the origin of the calc-alkaline magma series, and the formation of discordant dunite. Journal of Petrology 31, 51–98.

Kelemen, P.B., Dick, H.J.B., Quick, J.E., 1992. Formation of harzburgite by pervasive melt/rock reaction in the upper mantle. Nature 358, 635–641.

Kislov, E.V., Konnikov, E.G., Orsoev, D.A., Pushkarev, E.V., Voronina, L.K., 1997. Chlorine in the genesis of the low-sulfide PGE mineralization in the Ioko-Dovyrenskii layered massif. Geokhimya 5, 521–528 (Geochemistry International 35, 455–461).

Leblanc, M., 1991. Platinum-group elements and gold in ophiolitic complexes: distribution and fractionation from mantle to oceanic floor. In: Peters, T., Nicolas, A., Coleman, R.G. (Eds.), Ophiolite Genesis and Evolution of the Oceanic Lithosphere. Ministry of Petroleum and Minerals, Sultanate of Oman and Kluwer Academic Publishing, Dordrecht, pp. 231–260.

Leblanc, M., Ceuleneer, G., 1992. Chromite crystallisation in multicellular magma flow: evidence from a chromitite dike in the Oman ophiolite. Lithos 27, 231–257.

Leblanc, M., Nicolas, A., 1992. Ophiolitic chromitites. Chroniques de la Recherche Miniere 507, 3–25.

Leblanc, M., Violette, J.F., 1983. Distribution of aluminum-rich and chromium-rich chromite pods in ophiolite peridotites. Economic Geology 78, 293–301.

Lu, D.M., Hofmann, A.W., Rivalenti, R., Mazzucchelli, M., 1994. Geochemistry of the lower crustal mafic–ultramafic complex at Finero, Ivrea Zone, N. Italy. Goldschmidt Conference, Edinburgh, pp. 537–538.

Lu, M., Hoffmann, A.W., Mazzucchelli, M., Rivalenti, G., 1997a. The mafic–ultramafic complex near Finero (Ivrea–Verbano Zone): I. Chemistry of MORB-like magmas. Chemical Geology 140, 207–222.

Lu, M., Hoffmann, A.W., Mazzucchelli, M., Rivalenti, G., 1997b. The mafic–ultramafic complex near Finero (Ivrea–Verbano Zone): II. Geochronology and isotope geochemistry. Chemical Geology 140, 223–235.

Mathez, E.A., 1999. On factors controlling the concentrations of platinum group elements in layered intrusions and chromitites. In: Keays, R.R., Lesher, C.M., Lightfoot, P.C., Farrow, C.E.G. (Eds.), Dynamic Processes in Magmatic Ore Deposits and their Application in Mineral Exploration. Geological Association of Canada, Short Course, vol. 13, pp. 251–285.

McElduff, B., Stumpfl, E.F., 1990. Platinum-group minerals from the Troodos ophiolite, Cyprus. Mineralogy and Petrology 42, 211–232.

McInnes, B.I.A., Gregoire, M., Binns, R.A., Herzig, P.M., 2001. Hydrous metasomatism of oceanic sub-arc mantle, Lihir, Papua New Guinea; petrology and geochemistry of fluid-metasomatised mantle wedge xenoliths. Earth and Planetary Science Letters 188, 169–183.

McPherson, E., Thirlwall, M.F., Parkinson, I.J., Menzies, M.A., Bodinier, J.L., Woodland, A., Bussod, G., 1996. Geochemistry of metasomatism adjacent to amphibole-bearing veins in the Lherz peridotite massif. Chemical Geology 134, 135–157.

Medaris, L.G., 1975. Coexisting spinels and silicates in alpine peridotite of the granulite facies. Geochimica et Cosmochimica Acta 39, 947–958.

Melcher, F., Grum, W., Thalhammer, T.V., Thalhammer, O.A.R., 1999. The giant chromite deposits at Kempirsai, Urals: constraints from trace element (PGE, REE) and isotope data. Mineralium Deposita 34, 250–272.

Naldrett, A.J., Lehmann, J., 1988. Spinel non-stoichiometry as the explanation for Ni-, Cu- and PGE-enriched sulfides in chromitites. In: Prichard, H.M., Potts, P.J., Bowles, J.F.W., Cribb, S.J. (Eds.), Geo-Platinum 87 Symposium. Elsevier, London, pp. 93–109.

Naldrett, A.J., von Gruenewaldt, G., 1989. Association of platinum-group elements with chromitite in layered intrusions and ophiolite complexes. Economic Geology 84, 180–187.

Neal, C.R., 1988. The origin and composition of metasomatic fluids and amphiboles beneath Malaita, Solomon Islands. Journal of Petrology 29, 149–179.

Nicolas, A., Polino, R., Hirn, A., Nicolich, R., 1990. Ecors-Crop

traverse and deep structure of the western Alps. A synthesis. Memoires Geologiques de France 156, 15–27.

Roeder, P.L., Reynolds, I., 1991. Crystallization of chromite and chromium solubility in basaltic melts. Journal of Petrology 32, 909–934.

Roggiani, A.G., 1948. Ferro, cromo e platino nelle rocce basiche e ultrabasiche del Monte Gridone (Valle Vigezzo). Risveglio Ossolano, Domodossola, p. 32.

Stumpfl, E.F., 1986. Distribution, transport and concentration of platinum group elements. In: Gallagher, M.J., Ixer, R.A., Neary, C.R., Prichard, H.M. (Eds.), Metallogeny of Basic and Ultrabasic Rocks. Institution of Mining and Metallurgy, London, pp. 379–394.

Thayer, T.P., 1964. Principal features and origin of podiform chromite deposits, and some observations on the Guleman–Soridag district, Turkey. Economic Geology 59, 1497–1524.

Voshage, H., Hunziker, J.C., Hofmann, A.W., Zingg, A., 1987. A Nd and Sr isotopic study of the Ivrea Zone, Southern Alps, N-Italy. Contributions to Mineralogy and Petrology 97, 31–42.

Voshage, H., Sinigoi, S., Mazzucchelli, M., Demarchi, G., Rivalenti, G., Hofmann, A.W., 1988. Isotopic constraints on the origin of ultramafic and mafic dykes in the Balmuccia peridotite (Ivrea Zone). Contributions to Mineralogy and Petrology 100, 261–267.

Zanetti, A., Mazzucchelli, M., Rivalenti, G., Vannucci, R., 1999. The Finero phlogopite-peridotite massif: an example of subduction-related metasomatism. Contributions to Mineralogy and Petrology 134, 107–122.

Zhou, M.F., Robinson, P.T., 1997. Origin and tectonic environment of podiform chromite deposits. Economic Geology 92, 259–262.

Zhou, M.F., Robinson, P.T., Bai, W.J., 1994. Formation of podiform chromitites by melt/rock interaction in the upper mantle. Mineralium Deposita 29, 98–101.

Zhou, M.F., Sun, M., Keays, R.R., Kerrich, R.W., 1998. Controls on platinum-group elemental distribution of podiform chromitites: a case study of high-Cr and high-Al chromitites from chinese orogenic belts. Geochimica et Cosmochimica Acta 62, 677–688.